Correction for Ion Recombination in a Built-in Monitor Chamber of a Clinical Linear Accelerator at Ultra-High Dose Rates

Authors: Konradsson, Elise, Ceberg, Crister, Lempart, Michael, Blad, Börje, Bäck, Sven, et al.

Source: Radiation Research, 194(6) : 580-586

Published By: Radiation Research Society

URL: https://doi.org/10.1667/RADE-19-00012

RADIATION RESEARCH **194**, 580–586 (2020)
0033-7587/20 $15.00

DOI: 10.1667/RADE-19-00012

Correction for Ion Recombination in a Built-in Monitor Chamber of a Clinical Linear Accelerator at Ultra-High Dose Rates

Elise Konradsson,[a,1] Crister Ceberg,[a] Michael Lempart,[b] Börje Blad,[a,b] Sven Bäck,[a,b] Tommy Knöös[a,b] and Kristoffer Petersson[b,c]

[a] *Medical Radiation Physics, Department of Clinical Science, Lund University, Lund, Sweden;* [b] *Radiation Physics, Department of Hematology, Oncology and Radiation Physics, Skåne University Hospital, Lund, Sweden; and* [c] *The CRUK/MRC Oxford Institute for Radiation Oncology, Department of Oncology, University of Oxford, Oxford, United Kingdom*

Konradsson, E., Ceberg, C., Lempart, M., Blad, B., Bäck, S., Knöös, T. and Petersson, K. Correction for Ion Recombination in a Built-in Monitor Chamber of a Clinical Linear Accelerator at Ultra-High Dose Rates. *Radiat. Res.* 194, 580–586 (2020).

In the novel and promising radiotherapy technique known as FLASH, ultra-high dose-rate electron beams are used. As a step towards clinical trials, dosimetric advances will be required for accurate dose delivery of FLASH. The purpose of this study was to determine whether a built-in transmission chamber of a clinical linear accelerator can be used as a real-time dosimeter to monitor the delivery of ultra-high-dose-rate electron beams. This was done by modeling the drop-in ion-collection efficiency of the chamber with increasing dose-per-pulse values, so that the ion recombination effect could be considered. The raw transmission chamber signal was extracted from the linear accelerator and its response was measured using radiochromic film at different dose rates/dose-per-pulse values, at a source-to-surface distance of 100 cm. An increase of the polarizing voltage, applied over the transmission chamber, by a factor of 2 and 3, improved the ion-collection efficiency, with corresponding increased efficiency at the highest dose-per-pulse values by a factor 1.4 and 2.2, respectively. The drop-in ion-collection efficiency with increasing dose-per-pulse was accurately modeled using a logistic function fitted to the transmission chamber data. The performance of the model was compared to that of the general theoretical Boag models of ion recombination in ionization chambers. The logistic model was subsequently used to correct for ion recombination at dose rates ranging from conventional to ultra-high, making the transmission chamber useful as a real-time monitor for the dose delivery of FLASH electron beams in a clinical setup.

INTRODUCTION

FLASH radiotherapy is a novel technique by which radiation is delivered at ultra-high dose rates (>30 Gy/s), i.e., several orders-of-magnitude higher compared to conventional clinical radiotherapy beams (few Gy/min). Results from recently reported pre-clinical studies have demonstrated increased tolerance of the normal tissue (*1–3*) as well as similar tumor control for FLASH compared to conventional radiotherapy, i.e., an increased therapeutic window (*1, 4, 5*). With FLASH, the radioresistant tumors, which currently cannot be effectively treated with conventional radiotherapy, could potentially be treated at higher doses without an increased risk of normal tissue complications. The potential clinical benefits of this novel technique highlight the importance of translation from pre-clinical to clinical studies. To facilitate this translation, several technical and dosimetric challenges need to be resolved, such as enabling real-time output measurements to ensure accurate dose delivery (*6*).

Most studies investigating the FLASH effect have been performed using prototype research linear accelerators (*1–4, 7*). Due to the limited availability and high costs of these types of accelerators, only a few groups have studied the effect. However, researchers at Stanford University School of Medicine recently showed how a clinical linear accelerator (Clinac 21EX; Varian Medical Systems, Palo Alto, CA) can be adjusted to deliver FLASH beams (*8*), allowing more researchers to conduct FLASH studies. Inspired by this approach, our team of physicists and engineers was able to modify a linear accelerator from a different manufacturer (ELEKTA Precise, Stockholm, Sweden) to deliver electron beams with ultra-high dose rates (*9*). The beam is similar in energy to a clinical 10-MeV electron beam and is controlled on an electron pulse level. With a repetition frequency of 200 Hz, the modified linear accelerator in our clinic can achieve mean dose rates of $\geq$100 Gy/s at isocenter distance.

In order for FLASH treatment to be translated from pre-clinical studies to clinical trials, dosimetric studies are

[1] Address for correspondence: Lunds University, Barngatan 4, Skånes University Hospital, Lund 22185, Sweden; email: elise.konradsson@med.lu.se.

required to ensure accurate delivery of a prescribed dose. In conventional radiotherapy, the output of the linear accelerator is monitored and controlled using a built-in transmission ionization chamber, calibrated under reference conditions according to international dosimetry standards (*10*). However, at dose rates and dose-per-pulse (DPP) values beyond what is conventionally used, a drop-in ion-collection efficiency of the chamber can be observed, which presents a challenge to real-time dosimetry. Currently available methods to correct for the low-ion-collection efficiency of ionization chambers at ultra-high dose rates are not sufficient (*11*). Petersson *et al*. recently demonstrated how the drop-in ion-collection efficiency with increased DPP for an Advanced Markus chamber could be described with an empirical model created by fitting a logistic function to chamber measurements (*12*). We therefore hypothesize that by creating a similar model for the ion-collection efficiency of the transmission chamber in the clinical linear accelerator, the problem of low-ion-collection efficiency in the transmission chamber can be managed, allowing it to function as a real-time beam monitor for FLASH beams. Thus, the purpose of this work was to investigate if the transmission chamber in a clinical linear accelerator can be useful for real-time dosimetry at ultra-high dose rates, by measuring and modeling the ion-collection efficiency as the DPP increase from conventional values to FLASH values.

MATERIALS AND METHODS

The response from the built-in transmission ionization chamber (with the standard negative polarizing voltage of 320 V) in a clinical linear accelerator, modified for FLASH radiotherapy, was measured at dose rates ranging from conventional to ultra-high. Dose rates were controlled by adjusting the electron gun filament current. The dose rates and corresponding DPP values were measured with dose-rate-independent (*13*) Gafchromic™ EBT3 film (Ashland Specialty Ingredients G.P., Bridgewater, NJ), by positioning 3.3 × 3.3 cm^2 pieces one-by-one at dose maximum (2-cm depth) in a Solid Water HE phantom (Gammex Inc., Middleton, WI), at a source-to-surface distance (SSD) of 100 cm. Film analysis was performed using a flatbed scanner (Epson Expression 12000XL; Seiko Epson Corporation, Nagano, Japan) and ImageJ (version 1.52a, Wayne Rasband, NIH, Bethesda, MD), at 24 h postirradiation. Together with the transmission chamber reading, simultaneous measurements were performed with dose-rate-independent (*14*) LiF:Mg,Ti thermoluminescent dosimeters (TLD-100), a 0.6 cm^3 Baldwin-Farmer type ionization chamber (NE 2505/3-3A) and a clinical *in vivo* EDP 20-3G diode (IBA Dosimetry GmbH, Schwarzenbruck, Germany) to investigate their dose-rate dependence and to verify the film measurements. For each gun filament current setting, three sets of measurements were performed. The experiment was repeated with increased negative polarizing voltages (640 V and 960 V). Both the TLD and the film batch used for measurements were calibrated at a conventional dose rate against an ionization chamber (traceable to a standard laboratory) in a clinical 10-MeV electron beam, for a dose range of 1–30 Gy, using the same linear accelerator as for the DPP measurements.

Modified Clinical Linear Accelerator

A clinical ELEKTA Precise linear accelerator, temporarily modified to deliver ultra-high dose rates (*9*), was used for all measurements. An in-house-built electronic circuit, which enables the operator to control the output on a pulse-to-pulse basis, was connected to the accelerator. A diode (PIN-type, EDD 2-3G Diode, IBA Dosimetry GmbH), used as an electron beam pulse detector, was placed in the radiation field. The signal from the PIN diode was fed to the electronic circuit where it was converted to a voltage signal and then used as input signal to the interrupt pin of a microcontroller unit (MCU, Atmega328; Atmel Corporation, San Jose, CA). With the diode signal, the MCU was able to count the beam pulses and interrupt the accelerator when the desired amount of electron pulses had been delivered. The details regarding the modifications of the linear accelerator, e.g., the electronic circuit and how it interacts with the accelerator, can be found elsewhere by Lempart *et al*. (*9*).

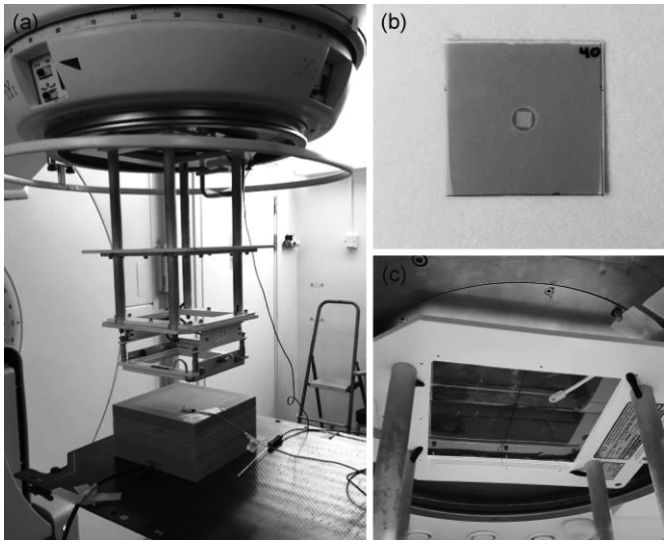

FIG. 1. Panel a: The measurement setup at a clinical linear accelerator. A solid water phantom was placed at SSD = 100 cm, with an *in vivo* diode at the top and a Baldwin-Farmer type ionization chamber at 9-cm depth. Film and thermoluminescent dosimeter (TLD) were positioned at 2-cm depth in the phantom, with a hole for TLD in one of the slabs (panel b). The PIN diode used as a pulse detector was positioned where the beam exits the treatment head (panel c).

Measurement Setup

The measurement setup (Fig. 1A) consisted of 10 cm of solid water slabs (20 × 20 cm^2) positioned on the treatment couch at an SSD of 100 cm, to mimic a clinical radiotherapy situation. The field size was defined by a 14 × 14 cm^2 electron applicator. In total, five dosimeters were used, including the built-in transmission ionization chamber. Gafchromic EBT3 film and TLD were placed in the center of the beam, at 2-cm depth inside the phantom (with a hole for TLD in one of the slabs) (Fig. 1B). To avoid the effect of ion recombination, the Baldwin-Farmer type ionization chamber (operated at –300 V of applied potential) was positioned at 9-cm depth in the phantom, also in the center of the beam. The ionization chamber was used in conjunction with a PTW UNIDOS electrometer (PTW-Freiburg, Freiburg, Germany) operated in charge mode. The clinical *in vivo* diode was placed at the top of the phantom at one of the radiation beam edges and connected to an APOLLO 5 electrometer (ONCOlog Medical QA AB, Uppsala, Sweden) operated in charge mode. To count the electron pulses, the PIN diode was positioned in the field where the beam exits the treatment head (at the cross-hair foil), without interfering with the other measurements (Fig. 1C). All measurements were performed simultaneously to remove any uncertainty added by output variation from the accelerator.

Response of Thermoluminescent Dosimeter, Ionization Chamber and Diode

The response of the TLD, the Baldwin-Farmer type ionization chamber and the *in vivo* diode was investigated at each of the measured DPP values. It was assumed that the ion recombination in the ionization chamber positioned at 9-cm depth in the phantom was negligible for all DPP values. To validate this assumption, the ion recombination correction factor for the ionization chamber, $k_{s,BF}$, was calculated for each gun filament current setting using the standard Boag two-voltage-analysis (TVA) (*10*):

$$k_{s,BF} = a_0 + a_1\left(\frac{M_1}{M_2}\right) + a_2\left(\frac{M_1}{M_2}\right)^2, \quad (1)$$

where a_0, a_1 and a_2 are constants defined by the voltage ratios (in our case, $a_0 = 1.198$, $a_1 = -0.875$, and $a_2 = 0.677$) and M_1 and M_2 are the measured collected charges (average of three measurements each) at polarizing voltages of 300 V and 100 V, respectively. For each gun filament current setting the polarity effect of the ionization chamber was measured and the polarity correction factor, $k_{pol,BF}$, was calculated according to:

$$k_{pol,BF} = \frac{|M_+| + |M_-|}{2|M_+|}, \quad (2)$$

where M_+ and M_- are the measured collected charges (average of three measurements each) at the positive and negative polarizing voltage of 300 V.

Transmission Chamber Response

The raw signal from one of the two existing monitor chamber channels was extracted from the linear accelerator and, after being reduced by a 2-Mohm (±1%) resistance, used as input signal for an electrometer (Elektra Precision electrometer; AB Mimator, Uppsala, Sweden). To control the polarizing voltage over the transmission chamber, an external high-voltage power supply (model 3102D; Canberra Industries Inc., Meriden, CT) was used. The absorbed dose (D) at 2-cm depth in the phantom can be related to the transmission chamber reading as shown by Technical Reports Series no. 398 (*10*):

$$D = M \cdot N \cdot k_{tp} \cdot k_h \cdot k_{elec} \cdot k_p \cdot k_s, \quad (3)$$

where M is the collected charge, N is a calibration coefficient, k_{tp} is the temperature and pressure correction factor, k_h is the humidity correction factor, k_{elec} is the electrometer correction factor, k_p is the polarity correction factor and k_s is the ion recombination correction factor. The polarity of the voltage applied over the transmission chamber was not shifted in the measurements and thus, k_p cannot be separated from k_s in Eq. (3). As the dose rate is varied, the calibration coefficient, temperature, pressure, humidity and electrometer correction factor are all constant, which means that the relative decrease in the signal from the transmission ionization chamber with increased DPP becomes a measure of the ion recombination at negative polarity. As k_s is assumed to be unity for conventional dose rates (*conv*), the ion-collection efficiency ($1/k_s$) can be calculated as:

$$\frac{1}{k_s} = \frac{M}{M_{conv}} \cdot \frac{D_{conv}}{D} \cdot \frac{N}{N} \cdot \frac{k_{tp}}{k_{tp}} \cdot \frac{k_h}{k_h} \cdot \frac{k_{elec}}{k_{elec}} = \frac{M}{M_{conv}} \cdot \frac{D_{conv}}{D}. \quad (4)$$

Ion-Collection Efficiency Models

A model of the ion-collection efficiency for an ionization chamber using pulsed radiation beams has been presented elsewhere by Boag (*15*):

$$\frac{1}{k_s} = \frac{1}{u}\ln(1+u), \quad (5)$$

where

$$u = \frac{\mu r d^2}{U}, \quad (6)$$

where μ is a constant that depends on the ionic recombination coefficient and ion mobilities, r is the initial uniform charge density of positive ions after a brief pulse of radiation (i.e., proportional to DPP), d is the chamber electrode spacing, and U is the applied chamber voltage. However, some of the electrons generated in the chamber may escape attachment to oxygen molecules and reach the collecting electrode of the chamber, resulting in an increase in ion-collection efficiency. This is known as the free electron component (p). To describe the ion recombination more accurately than Eq. (5), Boag *et al.* presented three extended models for plane-parallel ionization chambers, incorporating the free electron component (*11*):

$$\frac{1}{k_s'} = \frac{1}{u}\ln\left(1 + \frac{e^{pu} - 1}{p}\right), \quad (7)$$

$$\frac{1}{k_s''} = p + \frac{1}{u}\ln(1 + (1-p)u), \quad (8)$$

and

$$\frac{1}{k_s'''} = \lambda + \frac{1}{u}\ln\left(1 + \frac{e^{\lambda(1-\lambda)u-1}}{\lambda}\right), \quad (9)$$

where

$$\lambda = 1 - \sqrt{1-p}. \quad (10)$$

When considering a transmission chamber, the variables μ and d can add up to a constant c, reducing Eq. (6) to $u = (c \cdot DPP)/U$.

The different Boag models [Eqs. (5), (7)–(9)] were fitted to the data points from the transmission chamber response and DPP measurements, using GraphPad Prism version 8.0.0 for Windows (GraphPad Software, San Diego, CA)]. An empirical model was also created, by fitting a logistic function (*12*) to the data points, and compared to the Boag models.

RESULTS

Measurements in Dose Rates Ranging from Conventional to Ultra-High

The electron gun filament current was used to vary the DPP values. However, there was no linear correlation between the two. The electron gun filament current was gradually adjusted in 18 steps (step lengths ranging from 0.02–0.5 A) from the setting of conventional dose rates (~5.5 A) up to the value resulting in the highest output (~8 A) for each measurement series. The step lengths of the gun filament current were chosen such that the DPP values were somewhat equally distributed throughout the measured range. Mean dose rate at isocenter ranged from 0.1 Gy/s to 198 Gy/s (0.6 mGy < DPP < 0.99 Gy). Relative standard deviations (RSD) in measured output signal varied depending on the gun filament current setting, with large RSD in DPP (up to 30%) at points where the increase in output between two adjacent settings was large, and smaller RSD in DPP (<2%) at the setting producing the maximal output (i.e., the setting used for FLASH radiotherapy) where

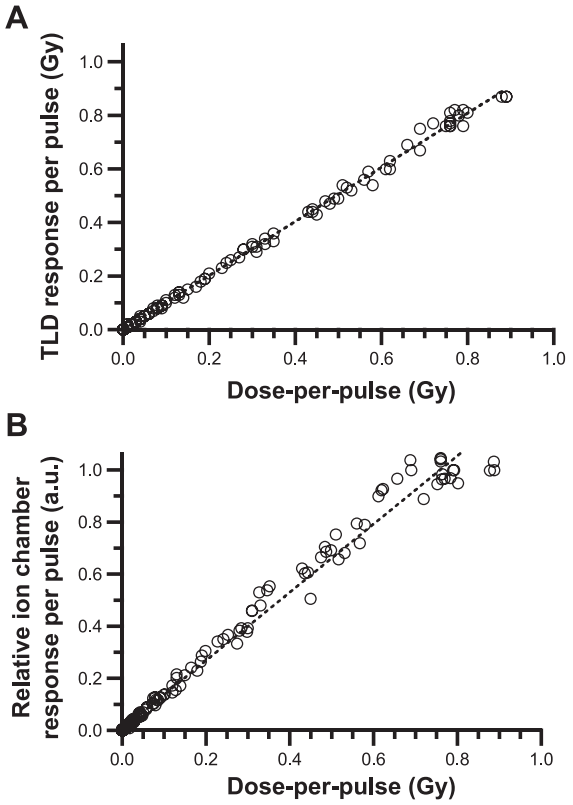

FIG. 2. The response per pulse was measured using the TLD (panel A) and a Baldwin-Farmer type ionization chamber (panel B), as a function of dose-per-pulse measured with radiochromic film. The response of the TLD and ionization chamber demonstrated a linear and a near-linear relationship with the film measurements, respectively.

the increase was less steep and consequently the output more stable.

TLD, Ionization Chamber and Diode Response

There was a linear agreement ($R^2 = 0.998$) between the measured TLD values and the radiochromic film measurements (Fig. 2A), verifying the dose-rate independence of TLD in our measured range as previously described (*14*). The mean absolute deviation between TLD and film measurements was 4% (range: 0–18%).

The TVA and polarization measurements (corrected for output variations) showed that values of $k_{s,BF}$ and $k_{pol,BF}$ were stable within uncertainties over the given DPP range. The relationship between the relative Baldwin-Farmer type ionization chamber response per pulse [corrected for temperature and pressure, ion recombination (using TVA) and polarity] and DPP (Fig. 2B) was linear up to approximately 0.7 Gy, after which a plateau was observed, indicating that there might be a dose-rate dependence for the chamber at this setup.

The *in vivo* diode response per pulse (Fig. 3) was linear up to DPP values of approximately 0.3–0.4 Gy, after which the diode saturated and no further notable increase in response per pulse with increased DPP could be measured.

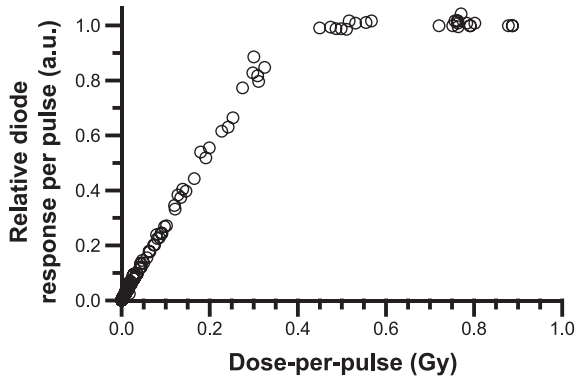

FIG. 3. The response per pulse was measured using an *in vivo* diode, as a function of dose-per-pulse measured with radiochromic film. The *in vivo* diode saturated at high dose-per-pulse values.

Transmission Chamber Response

The transmission chamber response for the negative polarizing voltages of 320 V, 640 V and 960 V all demonstrated that the ion-collection efficiency of the chamber decreased as the DPP increased (Fig. 4). A logistic function was fitted to the data points, thereby creating an empirical model of the ion recombination in the chamber:

$$\frac{1}{k_s} = \frac{1}{\left(1 + \left(\frac{DPP[mGy]\cdot 10}{U[V]}\right)^{\alpha}\right)^{\beta}}, \tag{11}$$

Where α and β are fitting constants and U is the negative polarizing voltage. The ion-collection efficiency goes towards 1 as the DPP goes towards 0, and the ion-collection efficiency goes towards 0 as the DPP goes towards ∞. The model is identical to the one presented by Petersson *et al.* for the Advanced Markus plane-parallel ionization chamber (PTW-Freiburg GmbH), with the exception of the factor 10 (*12*). R^2 value for the data points' position relative to the logistic function was 0.996, 0.999 and 0.997, for the negative polarizing voltages 320 V, 640 V and 960 V, respectively (Fig. 4A). The values of the fitting constants are shown in Table 1. The data points were also fitted using the four Boag models: one that does not incorporate the free electron component [Eq. (5)] and three that incorporate it in different ways [Eqs. (7)–(9)]. For the three latter models the fitted value of p was approximately zero (Table 2), and thus the resulting fits were close to identical for all four models, indicating that there is no free electron fraction. The R^2 value for the data points' position relative to the functions were 0.993, 0.976 and 0.978 for the negative polarizing voltages 320 V, 640 V and 960 V, respectively (Fig. 4B).

Transmission Chamber as a Real-Time Dose Monitor

For practical use of the transmission chamber, k_s is not known, and thus the DPP cannot be calculated directly from measurements using only the transmission chamber signal. Therefore, the recombination model is reformulated, to be a function of the apparent dose-per-pulse, DPP/k_s, a factor

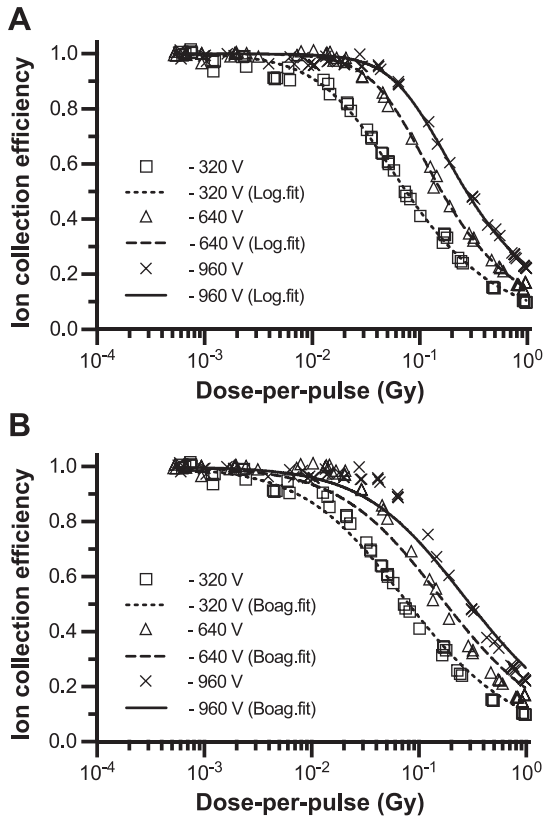

FIG. 4. Ion-collection efficiency of the transmission chamber as a function of dose-per-pulse according to simultaneous chamber and film measurements, for negative polarizing voltages of 320 V, 640 V and 960 V, together with (panel A) a logistic function [Eq. (11)] and (panel B) the theoretical Boag function [Eq. (5)] fitted to the data points.

that can be calculated from the transmission chamber signal:

$$\frac{1}{k_s} = \frac{1}{\left(1 + \left(\frac{DPP[mGy]}{k_s \cdot U[V]}\right)^{\gamma}\right)^{\delta}}, \tag{12}$$

where γ and δ are fitting constants and

$$\left(\frac{DPP}{k_s}\right) = \frac{M \cdot N \cdot k_{tp} \cdot k_h \cdot k_{elec}}{n}, \tag{13}$$

where n is the number of electron pulses. With this model, the ion recombination correction factor can be calculated directly from the transmission chamber signal, and the absorbed dose can be calculated using Eq. (3). Note that the transmission chamber must be calibrated against a dosimeter traceable to a standard laboratory at conventional dose rates, to determine the calibration coefficient N. This calibration, if performed in close connection to subsequent measurements at higher dose rates, will incorporate all factors in Eq. (3) apart from the monitor value and k_s. R^2 value for the data points' position relative to the logistic function [Eq. (12)] was 0.993, 0.993 and 0.996 for the negative polarizing voltages 320 V, 640 V and 960 V, respectively (Fig. 5). The values of the fitting constants are shown in Table 3.

TABLE 1
The Values of Fitting Constant α and β for a Logistic Function [Eq. (11)] Fitted to the Transmission Chamber Response, for Negative Polarizing Voltages of 320 V, 640 V and 960 V, respectively

	–320 V	–640 V	–960 V
α	1.35	1.92	1.94
β	0.486	0.360	0.322

TABLE 2
The Values of Fitting Constant *c* and the Free Electron Component *p* for Boag's Four Models of Ion-Collection Efficiency [Eqs. (5), (7)–(9)], for Negative Polarizing Voltages 320 V, 640 V and 960 V, respectively

	Eq. (5)	Eq. (7)	Eq. (8)	Eq. (9)
c (–320 V)	$9.98 \cdot 10^3$	$9.96 \cdot 10^3$	$9.98 \cdot 10^3$	$9.98 \cdot 10^3$
p (–320 V)	-	$1.99 \cdot 10^{-13}$	$5.24 \cdot 10^{-7}$	$5.04 \cdot 10^{-7}$
c (–640 V)	$8.98 \cdot 10^3$	$8.98 \cdot 10^3$	$8.96 \cdot 10^3$	$8.98 \cdot 10^3$
p (–640 V)	-	$2.67 \cdot 10^{-7}$	$5.95 \cdot 10^{-15}$	$2.61 \cdot 10^{-7}$
c (–960 V)	$8.01 \cdot 10^3$	$8.01 \cdot 10^3$	$8.00 \cdot 10^3$	$8.01 \cdot 10^3$
p (–960 V)	-	$2.72 \cdot 10^{-10}$	$4.55 \cdot 10^{-13}$	$3.32 \cdot 10^{-6}$

At a negative polarizing voltage of 320 V, the ion-collection efficiency at DPP = 0.98 Gy (i.e., the dose rate used for FLASH radiotherapy) was 0.1. By increasing the negative polarizing voltage to 640 V and 960 V, the ion-collection efficiency was increased by a factor 1.4 and 2.2, respectively. For the negative polarizing voltage of 320 V and 640 V, the logistic model [Eq. (12)] could not determine the ion recombination correction factor at the maximum DPP value with sufficient accuracy. In contrast, the logistic model for the negative polarizing voltage of 960 V could accurately determine the ion recombination correction factor, and the absorbed dose at the maximum DPP value could be calculated using Eq. (3) with a mean absolute deviation of 2.2% (range: 0.7–3.6%) from the dose measured with film.

DISCUSSION

Currently, transmission chamber-based dosimetry is required for all conventional clinical linear accelerators. However, because of the way the built-in transmission chambers are implemented in conventional radiotherapy and due to the drop-in ion-collection efficiency (*9*), they cannot be used for FLASH beams. In this study, the ion-collection efficiency of the built-in transmission chamber in a clinical linear accelerator was successfully modeled as a function of DPP. Our logistic model is similar to the model presented by Petersson *et al.* for the Advanced Markus plane-parallel ionization chamber (*12*). At the standard transmission chamber voltage of –320 V and at a polarizing voltage of –640 V, the ion-collection efficiencies at ultra-high dose

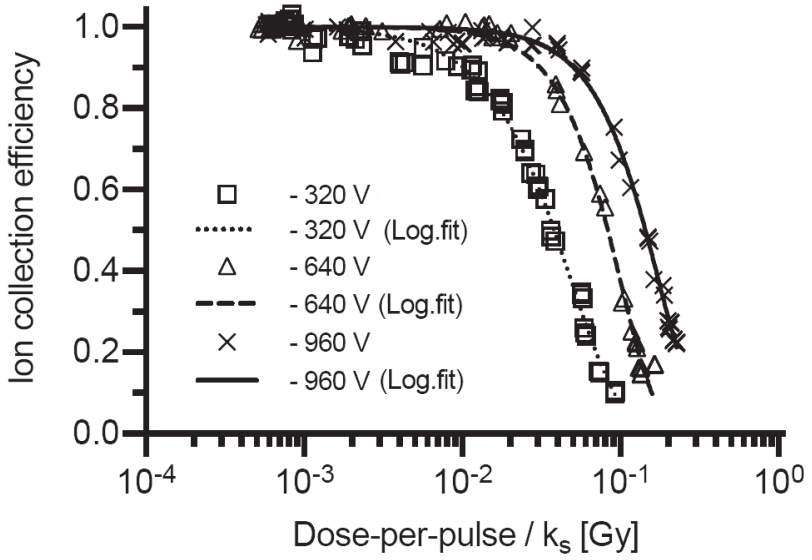

FIG. 5. Ion-collection efficiency of the transmission chamber as a function of DPP/k_s according to simultaneous chamber and film measurements, for negative polarizing voltages of 320 V, 640 V and 960 V, together with a logistic function (Eq. 12) fitted to the data points.

rates were too low to permit accurate dose determination with our model. However, at a polarizing voltage of –960 V, the recombination effect could be determined and the absorbed dose at the maximum DPP value could consequently be accurately calculated. We believe this study is an important step towards clinical implementation of FLASH radiotherapy (*5*).

The agreement between the four Boag models and the measured data describing the ion-collection efficiency as a function of DPP was rather poor. At high DPP (i.e., the region of highest interest for FLASH radiotherapy), the Boag models overestimated the ion-collection efficiency, whereas the empirical model fitted the data points accurately. These results are in line with previously published work in which it was reported that the Boag models are not accurate at high polarizing voltages (*12, 16, 17*). Therefore, the empirical model is preferred for monitoring beams with ultra-high dose rate. The four different Boag models were close to identical, and the free electron component was approximately zero for all three models incorporating it, indicating that there is no free electron fraction in transmission ionization chambers. Thus, these results suggest that in the calculation of the ion-collection efficiency of the transmission chamber, the free electron component is not relevant, and Boag's Eq. (5) behaves as Eqs. (7)–(9).

TABLE 3
The Values of Fitting Constant γ and δ for the Logistic Function of the Apparent Dose-per-pulse [Eq. (12)], for Negative Polarizing Voltages 320 V, 640V and 960 V, respectively

	–320 V	–640 V	–960 V
γ	1.44	1.87	1.82
δ	15.3	32.6	22.3

The dose results from the simultaneous measurements with TLD verified the dose results from the Gafchromic film measurements. As expected, TLD demonstrated to be dose-rate-independent in our experiment (*14*) and it was concluded that both film and TLD can be used as detectors at ultra-high dose rates. The ionization chamber (positioned at 9-cm depth in a solid water phantom) showed a tendency to saturate at DPP values >0.7 Gy. Thus, even with this setup, the ionization chamber appears to be of limited use for measurements in ultra-high dose-rate beams. The clinical *in vivo* diode saturated at DPP values of approximately 0.3–0.4 Gy and is therefore not appropriate as an *in vivo* detector in FLASH beams.

The approach to monitor the beam using the already existing built-in transmission chamber is very cost effective, because no new equipment is required. However, with our setup the beam is still controlled on a pulse level, which limits the accuracy of the dose delivery. One way to handle this would be by varying the gun filament current setting (with the transmission chamber as a dose monitor) to manipulate the amplitude of the pulse, thus receiving the desired dose for a certain amount of pulses. Further research is required to establish a more sophisticated way of controlling the beam delivery on a dose level. Ideally, the ion-collection efficiency model of the transmission chamber can be integrated in the MCU controller firmware. The raw transmission chamber signal could then be fed directly into the in-house electronic circuit, enabling interruption of the beam when the number of pulses corresponding to the desired dose has been delivered.

CONCLUSION

In this work we have presented a method to use the built-in transmission chamber of a clinical linear accelerator to monitor and measure ultra-high-dose-rate beams in a clinical setting. By increasing the transmission chamber's polarizing voltage and measuring the ion-collection efficiency as a function of dose-per-pulse, the recombination effect could be modeled and thereby taken into account, making the chamber useful for real-time dosimetry at ultra-high dose rates. This approach for real-time dose monitoring is now used when performing our pre-clinical experiments.

ACKNOWLEDGMENT

The research for this work was financially supported by Fru Berta Kamprads stiftelse.

Received: December 9, 2019; accepted: April 29, 2020; published online: June 22, 2020

REFERENCES

1. Favaudon V, Caplier L, Monceau V, Pouzoulet F, Sayarath M, Fouillade C, et al. Ultrahigh dose-rate FLASH irradiation increases the differential response between normal and tumor tissue in mice. Sci Transl Med 2014; 6:245ra93.
2. Montay-Gruel P, Petersson K, Jaccard M, Boivin G, Germond JF, Petit B, et al. Irradiation in a flash: Unique sparing of memory in mice after whole brain irradiation with dose rates above 100 Gy/s. Radiother Oncol 2017; 124:365–9.
3. Vozenin MC, De Fornel P, Petersson K, Favaudon V, Jaccard M, Germond JF, et al. The advantage of FLASH radiotherapy confirmed in mini-pig and cat-cancer patients. Clin Cancer Res 2019; 25:35–42.
4. Favaudon V, Fouillade C, Vozenin MC. Ultrahigh dose-rate, ''flash'' irradiation minimizes the side-effects of radiotherapy. (Article in French). Cancer Radiother 2015; 19:526–31.
5. Bourhis J, Montay-Gruel P, Goncalves Jorge P, Bailat C, Petit B, Ollivier J, et al. Clinical translation of FLASH radiotherapy: Why and how? Radiother Oncol 2019; 139:11–7.
6. Maxim PG, Keall P, Cai J. FLASH radiotherapy: Newsflash or flash in the pan? Med Phys 2019; 46:4287–90
7. Jaccard M, Duran MT, Petersson K, Germond JF, Liger P, Vozenin MC, et al. High dose-per-pulse electron beam dosimetry: Commissioning of the Oriatron eRT6 prototype linear accelerator for preclinical use. Med Phys 2018; 45:863–74.
8. Schüler E, Trovati S, King G, Lartey F, Rafat M, Villegas M, et al. Experimental platform for ultra-high dose rate FLASH irradiation of small animals using a clinical linear accelerator. Int J Radiat Oncol Biol Phys 2017; 97:195–203.
9. Lempart M, Blad B, Adrian G, Back S, Knoos T, Ceberg C, et al. Modifying a clinical linear accelerator for delivery of ultra-high dose rate irradiation. Radiother Oncol 2019; 139:40–5.
10. Andreo P, Burns DT, Hohlfeld K, Saiful Huq M, Kanai T, Laitano F, et al. Absorbed dose determination in external beam radiotherapy: An international code of practice for dosimetry based on standards of absorberd dose to water. Technical Reports Series No. 398. Vienna, Austria: International Atomic Energy Agency; 2000.
11. Boag JW, Hochhauser E, Balk OA. The effect of free-electron collection on the recombination correction to ionization measurements of pulsed radiation. Phys Med Biol 1996; 41:885–97.
12. Petersson K, Jaccard M, Germond JF, Buchillier T, Bochud F, Bourhis J, et al. High dose-per-pulse electron beam dosimetry - A model to correct for the ion recombination in the Advanced Markus ionization chamber. Med Phys 2017; 44:1157–67.
13. Jaccard M, Petersson K, Buchillier T, Germond JF, Duran MT, Vozenin MC, et al. High dose-per-pulse electron beam dosimetry: Usability and dose-rate independence of EBT3 Gafchromic films. Med Phys 2017; 44:725–35.
14. Karsch L, Beyreuther E, Burris-Mog T, Kraft S, Richter C, Zeil K, et al. Dose rate dependence for different dosimeters and detectors: TLD, OSL, EBT films, and diamond detectors. Med Phys 2012; 39:2447–55.
15. Boag JW. Ionization measurements at very high intensities. Pulsed radiation beams. Br J Radiol 1950; 23:601–11.
16. Burns DT, McEwen MR. Ion recombination corrections for the NACP parallel-plate chamber in a pulsed electron beam. Phys Med Biol 1998; 43:2033–45.
17. Gotz M, Karsch L, Pawelke J. A new model for volume recombination in plane-parallel chambers in pulsed fields of high dose-per-pulse. Phys Med Biol 2017; 62:8634–54.